NASA/TM—2018-219977

Optical Communication Link Assessment Utilizing a Modulated Retro-Reflector on Mars

Stephanie L. Booth and Robert M. Manning
Glenn Research Center, Cleveland, Ohio

November 2018

NASA STI Program . . . in Profile

Since its founding, NASA has been dedicated to the advancement of aeronautics and space science. The NASA Scientific and Technical Information (STI) Program plays a key part in helping NASA maintain this important role.

The NASA STI Program operates under the auspices of the Agency Chief Information Officer. It collects, organizes, provides for archiving, and disseminates NASA's STI. The NASA STI Program provides access to the NASA Technical Report Server—Registered (NTRS Reg) and NASA Technical Report Server—Public (NTRS) thus providing one of the largest collections of aeronautical and space science STI in the world. Results are published in both non-NASA channels and by NASA in the NASA STI Report Series, which includes the following report types:

- TECHNICAL PUBLICATION. Reports of completed research or a major significant phase of research that present the results of NASA programs and include extensive data or theoretical analysis. Includes compilations of significant scientific and technical data and information deemed to be of continuing reference value. NASA counter-part of peer-reviewed formal professional papers, but has less stringent limitations on manuscript length and extent of graphic presentations.

- TECHNICAL MEMORANDUM. Scientific and technical findings that are preliminary or of specialized interest, e.g., "quick-release" reports, working papers, and bibliographies that contain minimal annotation. Does not contain extensive analysis.

- CONTRACTOR REPORT. Scientific and technical findings by NASA-sponsored contractors and grantees.

- CONFERENCE PUBLICATION. Collected papers from scientific and technical conferences, symposia, seminars, or other meetings sponsored or co-sponsored by NASA.

- SPECIAL PUBLICATION. Scientific, technical, or historical information from NASA programs, projects, and missions, often concerned with subjects having substantial public interest.

- TECHNICAL TRANSLATION. English-language translations of foreign scientific and technical material pertinent to NASA's mission.

For more information about the NASA STI program, see the following:

- Access the NASA STI program home page at http://www.sti.nasa.gov

- E-mail your question to help@sti.nasa.gov

- Fax your question to the NASA STI Information Desk at 757-864-6500

- Telephone the NASA STI Information Desk at 757-864-9658

- Write to:
  NASA STI Program
  Mail Stop 148
  NASA Langley Research Center
  Hampton, VA 23681-2199

NASA/TM—2018-219977

Optical Communication Link Assessment Utilizing a Modulated Retro-Reflector on Mars

Stephanie L. Booth and Robert M. Manning
Glenn Research Center, Cleveland, Ohio

National Aeronautics and
Space Administration

Glenn Research Center
Cleveland, Ohio 44135

November 2018

Level of Review: This material has been technically reviewed by technical management.

Available from

NASA STI Program
Mail Stop 148
NASA Langley Research Center
Hampton, VA 23681-2199

National Technical Information Service
5285 Port Royal Road
Springfield, VA 22161
703-605-6000

This report is available in electronic form at http://www.sti.nasa.gov/ and http://ntrs.nasa.gov/

Optical Communication Link Assessment Utilizing a Modulated Retro-Reflector on Mars

Stephanie L. Booth and Robert M. Manning
National Aeronautics and Space Administration
Glenn Research Center
Cleveland, Ohio 44135

Summary

This work proposes the duplexing of an optical free-space (FS) communication link while minimizing the required power and complexity by using a modulated retro-reflector (MRR) within a system that is shown for a Mars orbiter and rover scenario. The MRR is placed on a planet's surface while the laser source is on the orbiter to achieve satellite communications with surface locations. The information, which varies from raw sensor data to multimedia files such as videos and other media, can be sent through this communication path. Due to the use of an MRR, an alternative modulating scheme is required to interpret a distorted signal. The arrangement suggested to prove the capabilities of the link is a nested pulse-position modulation (PPM) structure. A link budget was derived to show the link characteristics of this proposed system.

1.0 Introduction

Optical communication offers superior performance over radio frequency (RF) communication because the optical higher frequency carrier wave enables faster modulation rates and has a narrower beam divergence. The narrower beam divergence places more energy at the receiver for increased signal-to-noise ratios (*SNR*s) while facilitating the increased bandwidth. Nonetheless, the challenge of optical communications is that it requires two sources of power and beam control on both ends to achieve duplex communications. With current technology, a modulated retro-reflector (MRR) can eliminate one of these laser and pointing sources. For the scenario at hand, the laser is placed on an orbiter around Mars looking for communication with a rover on its surface, the second terminal. A MRR takes the laser and reflects the beam to return to its source along a parallel vector. Thus, the signal can be modulated on the downlink and uplink with a minimal amount of power, comparatively.

Using the suggested method may be the key to utilizing optical communications for future rovers and missions. MRRs bring the ability to have a duplex optical communication link. The importance of having a two-way link is that each second counts. The orbiter tends to lose sight of a surface unit due to the planet's rotation. For example, the Mars Reconnaissance Orbiter (MRO) only sees any given rover for approximately 73 min during a pass, according to an Analytical Graphics, Inc. (AGI) Systems Tool Kit® (STK) analysis, but only during about 16 of those 73 min, does communication happen. This is due to the angle the signal takes to get through the atmosphere. The further away from the rover's zenith angle, the more atmosphere the signal must travel through, giving more errors or requiring increased power output to reduce errors. Having a duplex link means that the full 16 min can be used for sending commands to the surface unit, and it can be used for sending all the information gathered to the orbiter.

To observe the performance of a system that utilizes a MRR, a link budget was generated based on existing research. In the proposed scenario, a laser modulated with pulse-position modulation (PPM) on an orbiter transmits toward the planet's surface to a MRR and a detector, the MRR identifies when it can modulate via the detector, and then the MRR returns the surface rover's pre-generated message back up to

the orbiter. This modulation scheme is simply based on on-off keying (OOK) and is used in this case in a binary mode, with one slot being zero and the other being a one. The link budget uses small steps to create the architecture that this scenario requires; however, the link budget can be taken and easily placed into different systems. The link budget was created in steps leading to separate categories: the initial power availability for the rover, finding the power for the uplink, and the communication performance of the links. Through this a basic optical communication link, the MRR properties for the link and nested PPM calculations can be found.

2.0 Two Optical Links for the Modulated Retro-Reflector (MRR) Communication System

There are two interconnected optical propagation links that must be controlled and analyzed properly to assure reliable communications from the orbiter to the rover on the surface of Mars and upon reflection from the MRR, back up to the orbiter. The required calculation commences with the basis of the benchmark analysis tool that NASA is now using for optical communications, that is, the Link Assessment Tool of the Space Communications and Navigation (SCaN) Project (Ref. 1). The individual components that enter into such communications link calculations will now be reviewed and more detailed information than given below can be found in Reference 1.

2.1 Power for Initial Downlink to Mars Rover

2.1.1 Satellite Effective Isotropic Radiated Power (*EIRP*)

In this case, the *EIRP* is a measure of the total power transmitted by the optical laser transmitter on the orbiter. It is defined by the product of the output power of the laser source, P_T, in watts, the orbiter transmitter aperture gain, G_T, and the total optical losses in the transmitter, τ_T. Since the optical losses, τ_T (or losses in general), are usually stated in units of dB, it is necessary to convert this specification to a multiplicative loss by using the relation $10^{\tau_T/10}$. The *EIRP* (in watts) of the optical transmitter is then given by

$$EIRP = P_T G_T 10^{\tau_T/10} \tag{1}$$

The orbiter transmitter aperture gain is constrained by the transmitted beam divergence angle, θ_{div} (in radians), and is defined by

$$G_T = \frac{8}{\theta_{div}^2} \tag{2}$$

However, the beam divergence angle can be calculated from the operating laser wavelength, λ (in meters), and the orbiter transmitter aperture diameter, D_T (in meters). This results in the beam divergence angle of the transmitted beam, given by

$$\theta_{div} = \sqrt{8}\frac{\lambda}{\pi D_T} \tag{3}$$

2.1.2 Free-Space (FS) Path Loss

The signal energy transfer out of the orbiter, as captured in the *EIRP* metric, must now be transmitted through space down to the surface of Mars to serve two purposes: to be captured by the optical receiver

on the rover to convey tracking and control information to the rover and to provide for the optical power to the MRR for subsequent modulation and retransmission back up to the orbiter. The transmission through space incurs a loss mechanism that is associated with the natural diffractive spreading of the optical beam leaving the transmitter. This spreading is responsible for the famous $1/r^2$ loss where r is the distance traveled. Letting *Rng* (in meters) be the range from the laser transmitter on the orbiter to the sensors on the Mars rover, the FS path loss is given by

$$L_{\mathrm{FS}} = \left(\frac{\lambda}{4\pi Rng} \right)^2 \tag{4}$$

In addition to the FS loss, another loss occurs by the absorption and scattering of the optical radiation within the Martian atmosphere. Now, the wavelength dependent parameter, $\overline{\tau_{\mathrm{atm}}}$, that is a measure of the atmospheric absorption and scattering, is constant for a given wavelength and assumes the distance is measured normal to the surface. Although, any propagation path that occurs at an angle θ from this line into space will experience an absorption of $\tau_{\mathrm{atm}}(\theta) > \overline{\tau_{\mathrm{atm}}}$ due to the geometrical extension of the path distance. Hence, the loss mechanism connected with the process of molecular absorption and scattering is represented by

$$\tau_{\mathrm{atm}}(\theta) = \frac{\overline{\tau_{\mathrm{atm}}}}{\sin(\theta)} \tag{5}$$

and from now on $\tau_{\mathrm{atm}}(\theta)$ will be noted as τ_{atm}. Since this parameter is usually given as a loss measured in decibels, its incorporation into the power flow analysis here is given by $10^{\tau_{\mathrm{atm}}/10}$. At the wavelength used in this scenario of 1,550 nm, a typical value for the Martian atmosphere is $\overline{\tau_{\mathrm{atm}}} = 0.72$ dB.

2.1.3 Optical Power Available on the Surface of Mars

Finally, an expression for the resulting optical communication power available on Mars surface to the rover and retro-reflection back up to the orbiter can be obtained. The power available is simply given by

$$P_{\mathrm{Mars}} = EIRP\, L_{\mathrm{FS}} 10^{\tau_{\mathrm{atm}}/10} \tag{6}$$

This optical power that is available on the surface of Mars will now be used for two purposes: to establish a downlink from the orbiter directly with the rover for control purposes and to provide an optical source field that can be reflected from an MRR mounted on the rover back up to the orbiter. The MRR will impart further modulation onto the optical field, essentially overlaid on the signal from the downlink on the orbiter, to carry science information as well as telemetry and tracking data back to the orbiter.

2.1.4 Detected Optical Signal Power for Communications To and From Rover

2.1.4.1 Gain of Rover Optical Receiver

The expression used to calculate the received gain of the downlink detector associated with the optical receiver is given for a typical downlink detector aperture diameter, D_{det}, and is defined as

$$G_{\mathrm{det}} = \left(\frac{\pi D_{\mathrm{det}}}{\lambda} \right)^2 \tag{7}$$

2.1.4.2 Downlink Optical Power

For the purposes of this paper, 1 represents downlink and 2 represents uplink in symbols. The detected optical signal power (in watts) of the downlink detector, $P1_s$, placed behind the receiver aperture can be found by the quantum efficiency of the downlink detector on the rover, η_{det1}, the received gain of the downlink detector, and the communication power available on the Martian surface, P_{Mars}. The relationship is given by

$$P1_s = \eta_{det1} G_{det} P_{Mars} \tag{8}$$

This particular downlink power will be directly used in the subsequent calculations for the modulation-type dependent communication performance metrics for the orbiter-to-rover communications link, such as the bit error rate (BER) and channel capacity (C). The operation of the retro-reflected optical signal from the MRR to the orbiter must now be considered.

2.1.4.3 Gain of Rover Modulated Retro-Reflector (MRR)

Similar to that of Equation (7), the receive gain of the MRR aperture of diameter, D_{MRR}, is given by

$$G\text{rec}_{MRR} = \left(\frac{\pi D_{MRR}}{\lambda} \right)^2 \tag{9}$$

In the event that more than one MRR is used to generate an uplink back to the orbiter, the gain can change. With N_{MRR} being the number of MRRs on the rover, the associated gain is now given by

$$G\text{rec}_{MRR} = \left(\frac{\pi D_{MRR}}{\lambda} \right)^2 N_{MRR} \tag{10}$$

2.1.4.4 Source Uplink Optical Power

Since this system requires the use of a retro-reflector, which is an array of mirrors organized to reflect the received optical light at the same angle as it was received, there are reflective properties that need to be accounted for. The reflective surface properties of the MRR are captured by the use of the Strehl ratio, S_R, which is representative of a surface roughness factor σ_λ; it is this dimensionless roughness parameter that establishes the reflectivity of the surface as the fraction of incident optical radiation that is retransmitted from the surface. This ratio is given by Reference 2 as

$$S_R = 1 - (2\pi\sigma_\lambda^2) \tag{11}$$

The MRR transmitted signal power, $P\text{mrr}_T$, can now be related to the communication power available on Mars' surface, P_{Mars}, by

$$P\text{mrr}_T = S_R G\text{rec}_{MRR} P_{Mars} \tag{12}$$

Unlike the similar quantity found by Equation (8), which is used to find communications integrity of the downlink, the result of Equation (11) provides the initial power for the optical uplink to the orbiter.

2.2 Power for Uplink Back to Mars Orbiter

2.2.5 Optical Power Available at Orbiter

The analysis of the second communication link, whose initial power source is $P\text{mrr}_T$, as opposed to the *EIRP* of Equation (1), now follows along the exact same lines as the development for the downlink given by Equations (4) to (6). Following the same logic, the communication power available on the Mars orbiter is now given by

$$P_{\text{orb}} = P\text{mrr}_T L_{\text{FS}} 10^{\tau_{\text{atm}}/10} \tag{13}$$

where τ_{atm} is actually linear in the equation, but the user specification is in decibels. Therefore, the conversion was made.

2.2.6 Gain of Orbiter Optical Receiver

With D_{orb} as the orbiter detector aperture diameter (in meters), the receive gain of the orbiter detector is given by

$$G_{\text{orb}} = \left(\frac{\pi D_{\text{orb}}}{\lambda} \right)^2 \tag{14}$$

2.2.7 Uplink Optical Power

The efficiency detector of the optical detector, η_{det2}, in the orbiter receiver leads to the detected optical signal power on the orbiter (in watts). Therefore, the output from the optical detector leads to the detected optical signal power (in watts) on the orbiter that is output from the optical detector placed behind the receiver aperture on the orbiter given by

$$P2_s = \eta_{\text{det}\,2} G_{\text{orb}} P_{\text{orb}} \tag{15}$$

Like Equation (8) for the downlink power to the rover, Equation (15) gives the uplink power that will be directly used in the subsequent calculations for the communication performance metrics for the rover-to-orbiter communications link. These considerations will now follow for the communication modulation format of PPM.

2.3 Signal Performance Supported for Both Downlink and Uplink

Before the link performance characteristics of BER and *C* can be obtained for the communication links as defined above, it is first necessary to convert all the optical power quantities into the equivalent number of photon flux they represent. Additionally, the power (or photon) flow will be modulated by some technique to impart information onto the optical wave field. In this application, PPM will be used, whereby the intensity of the optical field is keyed using on-off states of the intensity, as in the power flow. The time interval, *T*, of these on-off states is determined by the data rate, *Rb*, conveyed over the optical link, an example being the rate at which the on-off states of power are cycling. This is also known as the slot width, which is a PPM slot, representing the PPM index, *M* (refer to Appendix B).

The two power parameters that are of interest here are detected optical signal power of the downlink detector, $P1_s$, and the detected optical signal power on the orbiter, $P2_s$, resulting from the modulated retro-reflected wave field from the MRR. The uplink signal is seen at the output of the receiver detector on the

orbiter. In order to convert these into their corresponding numbers of photons, K, consider the fact that if the power, P (in watts), contained in the wave field is measured over a slot time interval, T (in seconds), by a detector, there are

$$K = \frac{\lambda P}{\mathrm{h\ c}} T \tag{16}$$

photons captured by the detector. Because the PPM data structure will be different for the downlink from the orbiter compared to the uplink back to the orbiter, each case must be considered separately. This allows the appropriate functional relationship between the slot time interval, T, and the prevailing data rate.

2.3.8 Pulse-Position Modulation of Order 2 (PPM2) Downlink From Orbiter

2.3.8.1 Number of Photons in Signal and Background Noise

The optical downlink from the orbiter will use PPM of order 2, meaning a PPM data format in which two message bits are encoded onto a word within the optical field emanating from the transmitter laser. The downlink will have a data rate of Rb_1 and recall for a PPM2 case that there is a PPM index, denoted by M_1, of 2, where M_1 is designated for the downlink. For a basic PPM slot structure of index M, under ideal circumstances, M and T can be combined for the temporal width, MT, of a symbol of a M-order PPM frame given by

$$M * T = \frac{\log_2(M)}{Rb} \tag{17}$$

However, to account for dead time that may exist between PPM symbols due to delays in the laser transmitter response, and so forth, Equation (17) is appended with a guard time interval T_G (Ref. 3) such that

$$MT + T_G = \frac{\log_2(M)}{Rb} \tag{18}$$

Thus, in the case considered for a data rate, Rb_1, for the downlink from the orbiter and letting $M = M_1$, the corresponding slot time interval $T = T_{S1}$ for a PPM slot with a guard time is given by

$$T_{S1} = \frac{1}{M_1}\left(\frac{\log_2(M_1)}{Rb_1} - T_G\right) \tag{19}$$

Hence, by Equation (16), the number of photons per slot, K_{S1}, contained within the detected optical signal power of the downlink detector, $P1_s$, is given by

$$K_{S1} = \frac{\lambda P1_s}{\mathrm{h\ c}} T_{S1} \tag{20}$$

where c is the speed of light and h is Planck's constant.

The signal photons that enter into the optical detector on the rover are not the only photons that need to be considered. The key to the calculations that ultimately yield communication link performance metrics such as the BER and channel capacity is the ability to compare the power, or, in this case, the number of photons that characterize the signal, to the power (or number of photons) that characterizes any other source or sources that do not support communications. These other noncommunication sources constitute the noise environment in which the process of detection of the signal must take place (Refs. 4

and 5). Thus, a relationship analogous to that of Equation (20) must be employed to calculate the prevailing noise photons, for example, any photons entering the link that do not directly support communications. For the communication scenario addressed here, there are two potential sources of noise photons: those that come from the brightness of the Mars sky during daytime hours (the sky radiance) and those that come from the reflection of the Sun from the surface of the planet (the planetary radiance). Both of these sources of radiation combine into an overall irradiance term I_{Rad} (in units of W/m²/°/s). The use of this specification involves the field-of-view (FOV) of the receiver aperture, Ω_{FOV}, the downlink detector aperture diameter itself, D_{det}, as well as the value associated with the optical filter noise bandwidth, B_F, that is added to the aperture of the receiver to help filter out radiation that is not of the specific wavelength being used by the optical transmitter (in this case, 1,550 nm). All of these parts are combined to give the optical background power for the downlink, $P1_b$ (in watts), from the ambient radiation as seen by the optical detector on the rover (Refs. 4 and 5)

$$P1_b = I_{Rad} B_F \Omega_{FOV} \left(\frac{\pi D_{det}^2}{4} \right) \eta_{det1} \tag{21}$$

and the FOV (in Steradians) of the receiver aperture, given by

$$\Omega_{FOV} = \pi \left(2 \frac{2.44\lambda}{D_{det}} \right)^2 \tag{22}$$

Given these developments, the calculated noise field that enters the rover's detector within the slot time interval, T_{S1}, can now be obtained as

$$K_{b1} = \frac{\lambda P1_b}{\mathrm{h\ c}} T_{S1} \tag{23}$$

It is the comparison of the photon rates given by Equations (20) and (23) that ultimately determines the BER that prevails for digital communication on the downlink from the orbiter as well as the important channel capacity of the link. This ultimately determines the maximum data rate that the channel can support.

2.3.8.2 Bit Error Rate (BER) and Channel Capacities for Downlink

The calculation of the BER that the digital communication link will incur upon traversing the downlink from the orbiter commences with the consideration of the corresponding *SNR*. The value of which is determined (Ref. 6) by the signal and background noise photons considers above, that is,

$$SNR_1 = \left(\frac{M_1 K_{S1}}{\sqrt{F_1 M_1 K_{S1} + K_{b1}} + \sqrt{K_{b1}}} \right)^2 \tag{24}$$

which directly determines the probability of the PPM bit error in FS (Ref. 6)

$$Pbf = \frac{1}{2} erfc \left[\frac{1}{4} \sqrt{M_1 \log_2(M_1) SNR_1} \right] \tag{25}$$

where *erfc* is the complementary error function. The quantity F_1 appearing in Equation (24) is the downlink avalanche photodiode noise figure used on the rover to intercept the downlink from the orbiter; in the case of an avalanche photodiode (APD), it is specified with the downlink ionization factor of the APD, ζ_1, and the downlink APD gain factor, E_1, and is given by

$$F_1 = 2 + \zeta_1 E_1 \tag{26}$$

The channel capacity for the PPM downlink is also associated with the signal and noise photons through the relationship

$$C_{\mathrm{PPM}}(\mathrm{bit/s}) = \frac{1}{T_S}\left[\left(K_S + \frac{K_n}{M}\right)\log_2\left(1 + \frac{MK_S}{K_n}\right) - \left(K_S + K_n\right)\log_2\left(1 + \frac{K_S}{K_n}\right)\right] \tag{27}$$

where T_S is symbol duration, K_S is the average number of the detected signal, and K_n is the average number noise. Both the coded and uncoded power margins that prevail on the link can be found using this prescription. Thus, for the case of the downlink from the orbiter, the channel capacity needed to support the required data rate is simply $C_{\mathrm{PPM}} = Rb_1$. For the average number noise of photons per slot value found earlier, $K_n = K_{b1}$ in Equation (27) as well as $T_S = T_{S1}$. This then gives the relation

$$Rb_1 = \frac{1}{T_{S1}}\left[\left(K_S + \frac{K_{b1}}{M_1}\right)\log_2\left(1 + \frac{M_1K_S}{K_{b1}}\right) - \left(K_S + K_{b1}\right)\log_2\left(1 + \frac{K_S}{K_{b1}}\right)\right] \tag{28}$$

where T_{S1} is the slot period. If this relation is solved for the average number of the detected signal, K_S, this explains the required number of photons needed by the channel to support the required data rate Rb_1. Thus, solving Equation (28) for K_S with the calculated noise field K_{b1} gives the correspondingly required photon flux that the receiver needs to see in order to close the link and receive the modulated data (Ref. 1). From this, and comparing it to the actual photon flux at the receiver from power considerations, the uncoded link power margin is obtained. Additionally, by letting $K_{b1} \to 0$ in Equation (28), a solution can be obtained (Ref. 1) in the case of a noiseless channel whereby a value for K_S will represent a coded channel, on the assumption that available coding techniques allow for approach to a noiseless channel. Thus, a photon flux is obtained for a noiseless or coded channel by supporting a data rate of Rb_1 margin.

2.3.9 Pulse-Position Modulation of Order 4 (PPM4) Uplink From Rover

2.3.9.1 Number of Photons in Signal and Background Noise

The power source for the optical uplink from the rover back up to the orbiter is provided by the reflected optical radiation from the MRR mounted on the rover. Since the MRR is a completely passive device that does not provide additional power to the reflected link, it modulates the reflected radiation field by dynamically adjusting its reflection coefficients (Ref. 2). Therefore, the MRR can only modulate the optical radiation field when the PPM downlink stream is in an on state. Since an off state does not contain a power density to reflect, the MRR must necessarily modulate the reflected signal used in the uplink by using a higher order PPM signaling format like a PPM4 data format. The PPM slot structure of the uplink is necessarily connected with that of the PPM slot structure on the downlink. The slot timing considerations of Equations (17) to (19) now become more intricate. Equation (18) is used once again but now with different constraints. In general, when a M_2 order PPM signal is embedded upon a M_1 order PPM data stream, as happens with the MRR, the temporal length $M_1T_{S1} + T_G$ of the original frame

structure prevails and becomes connected to that of the nested PPM structure, $\frac{\log_2(M_2)}{Rb}$, through a variation of Equation (18),

$$M_1 T_{S1} + T_G = \frac{\log_2(M_2)}{Rb} \tag{29}$$

where M_1 is the PPM index for the downlink and M_2 is the PPM index for the uplink. However, the associated data rate, *Rb*, unlike that of the downlink, which is a freely determined quantity, now becomes governed by the constraint of Equation (29). Hence, letting $Rb = Rb_2$ be this uplink data rate, Equation (29) requires that

$$Rb_2 = \frac{\log_2(M_2)}{M_2 T_{S2} + T_G} \tag{30}$$

where

$$T_{S2} = \left(T_{S1} M_1 / M_1\right) \tag{31}$$

is the slot time interval for the nested uplink signal. Equations (30) and (31), in addition to Equation (15), show that the available power received at the orbiter is sufficient to now employ the same procedure used for the uplink power budget in Section 2.3.8 but for a PPM4 link. Therefore, the corresponding number of photons at the orbiter optical detector is given by

$$K_{S2} = \frac{\lambda P2_s}{\mathrm{hc}} T_{S2} \tag{32}$$

The noise power on the uplink will predominantly come from solar reflection and the Mars surface radiance, $I_{Rad\mathrm{MS}}$, and thus the background power for the uplink is given by

$$P2_b = I_{Rad\mathrm{MS}} B_{\mathrm{F}} \Omega_{\mathrm{FOV}} \left(\frac{\pi D_{\mathrm{orb}}^2}{4}\right) \eta_{\mathrm{det}\,2} \tag{33}$$

where D_{orb}^2 can be written as $(D_{\mathrm{orb}}*10^2)^2$ to unit match with the units of $I_{Rad\mathrm{MS}}$ and the FOV of the receiver aperture (in steradians) is given by

$$\Omega_{\mathrm{FOV}} = \pi\left(2\frac{2.44\lambda}{D_{\mathrm{orb}}}\right)^2 \tag{34}$$

Finally, the corresponding photon flux from the noise background is

$$K_{b2} = \frac{\lambda P2_b}{\mathrm{hc}} T_{S2} \tag{35}$$

2.3.9.2 Bit Error Rate (BER) and Channel Capacities for Uplink

As with Section 2.3.9.1, everything follows from the previous considerations in Section 2.3.8.2, for,

$$SNR_2 = \left(\frac{M_2 K_{S2}}{\sqrt{F_2 M_2 K_{S2} + K_{b2}} + \sqrt{K_{b2}}} \right)^2 \tag{36}$$

where F_2 is the orbiter avalanche photodiode noise figure, with the corresponding FS BER

$$Pbf = \frac{1}{2} erfc\left[\frac{1}{4} \sqrt{M_2 \log_2 (M_2) SNR_2} \right] \tag{37}$$

the channel capacity characteristics follow from the relation

$$Rb_2 = \frac{1}{T_{S2}} \left[\left(K_S + \frac{K_{b2}}{M_2} \right) \log_2 \left(1 + \frac{M_2 K_S}{K_{b2}} \right) - (K_S + K_{b2}) \log_2 \left(1 + \frac{K_S}{K_{b2}} \right) \right] \tag{38}$$

3.0 Assessment Flowchart

This section contains a flowchart (Figure 1 to Figure 7) of the MRR communications system link assessment.

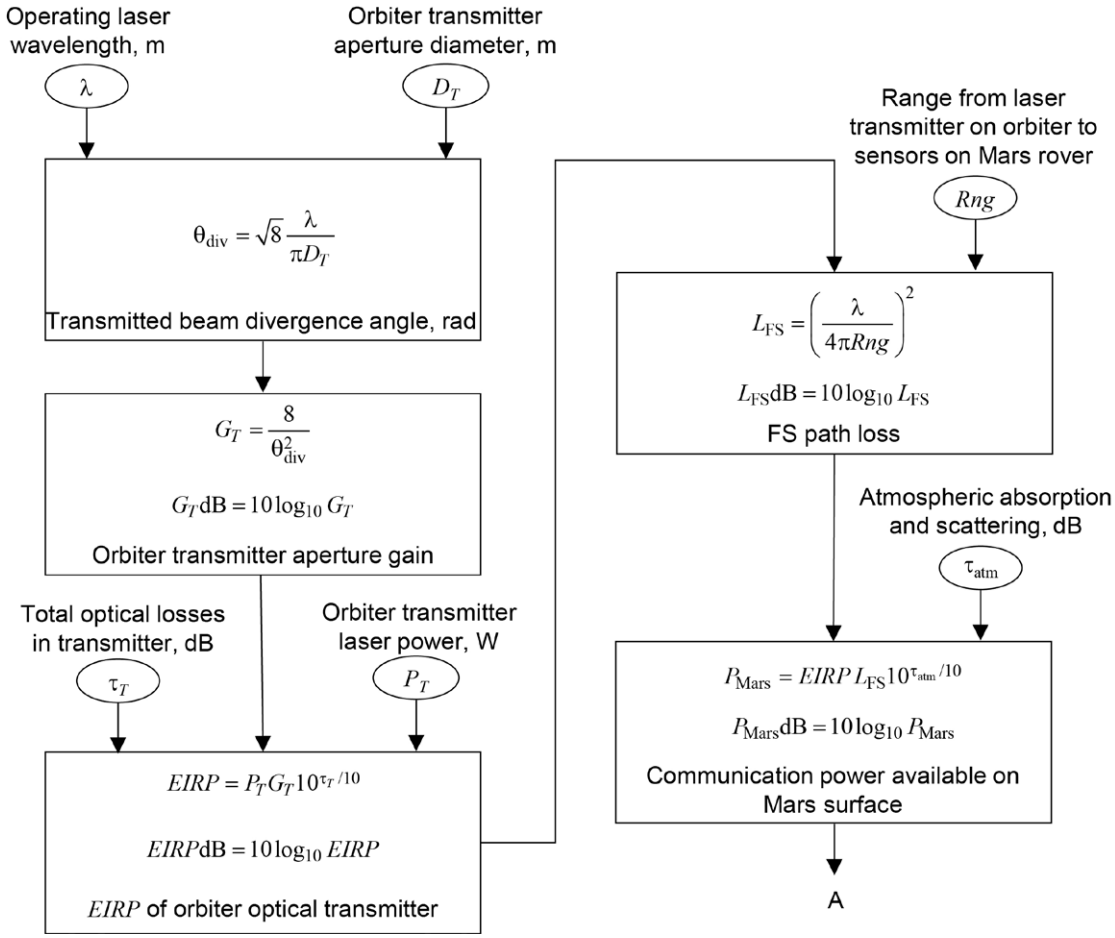

Figure 1.—Initial power gains and losses to surface of Mars from laser source.

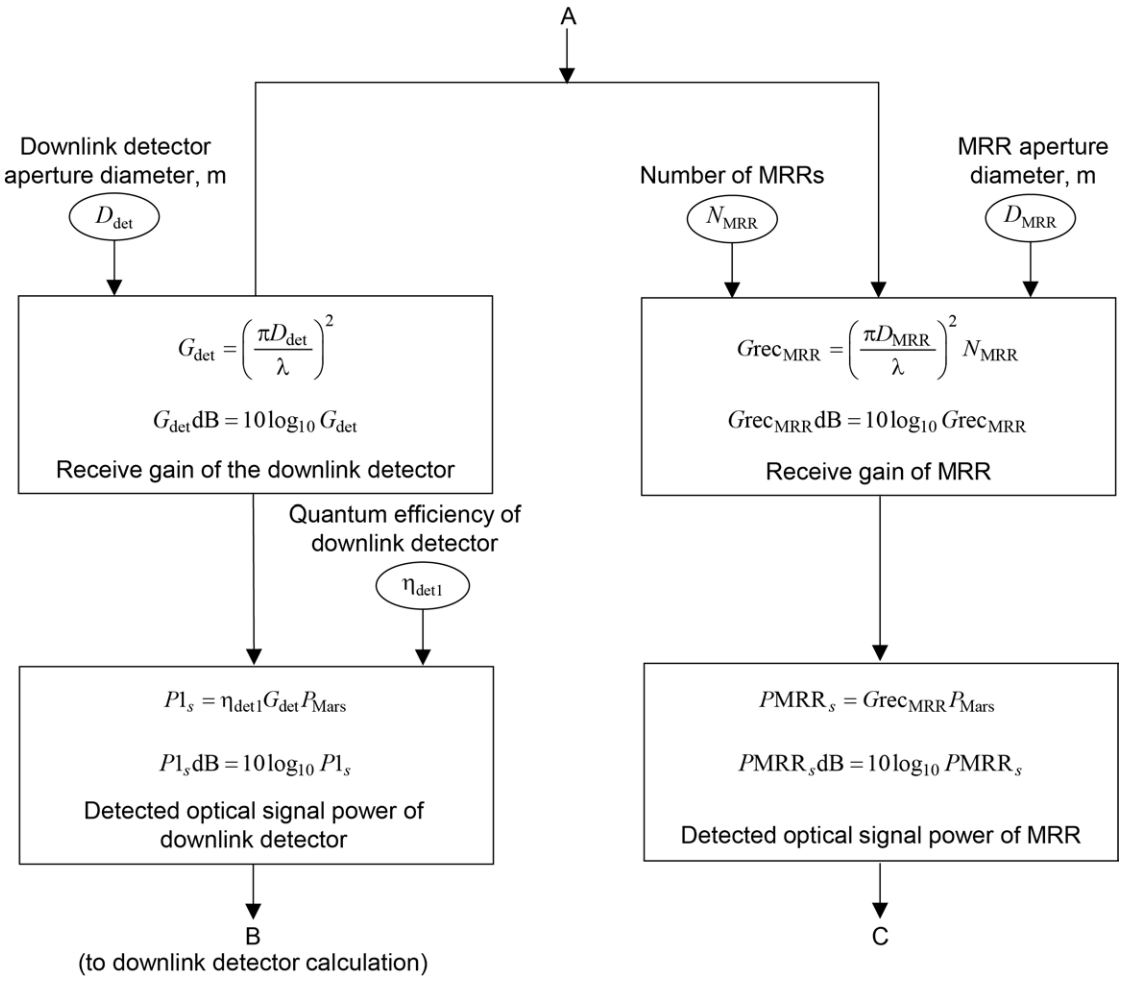

Figure 2.—Detected amount of power for devices on Mars surface.

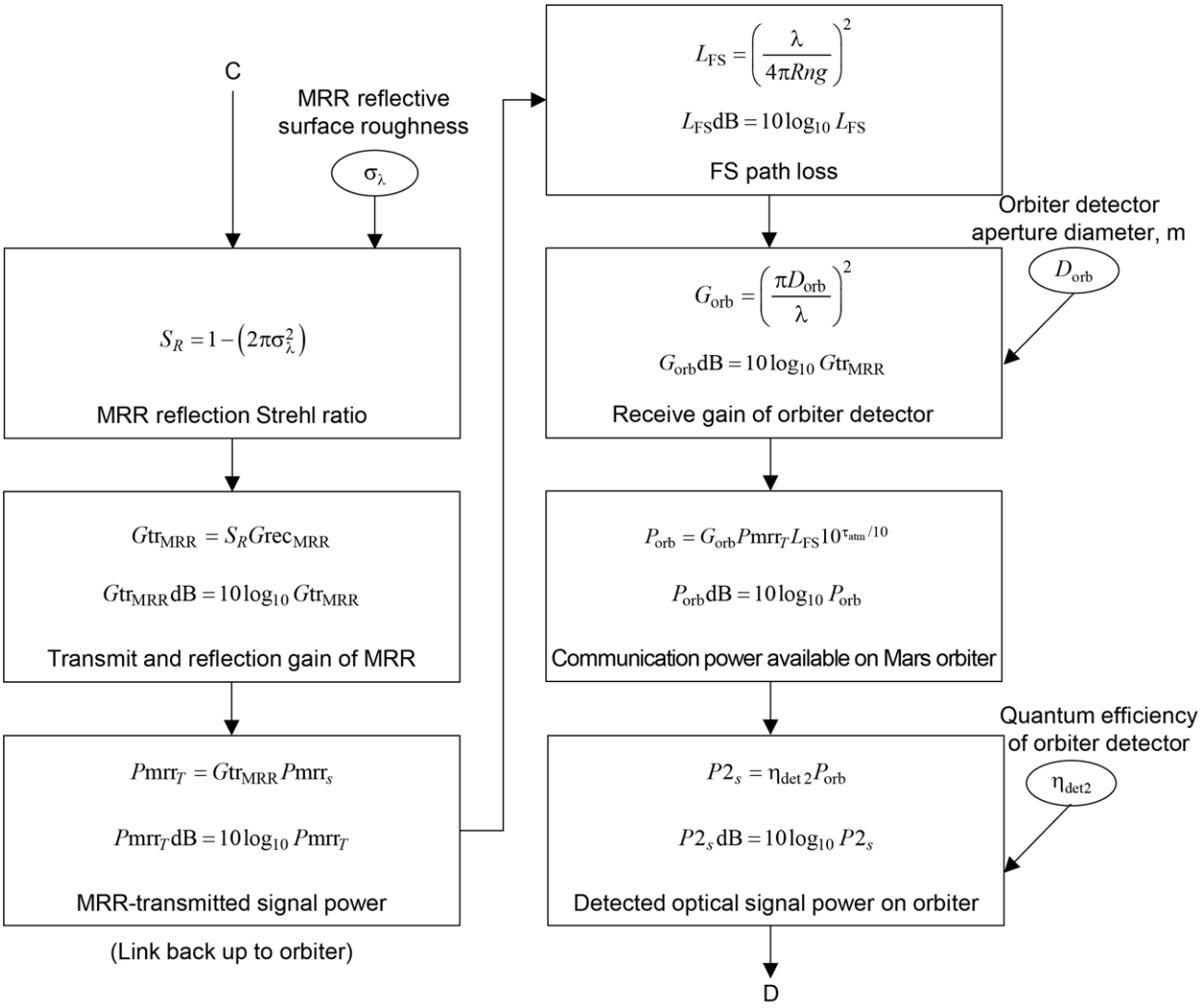

Figure 3.—Return link to orbiter with MRR gains and losses.

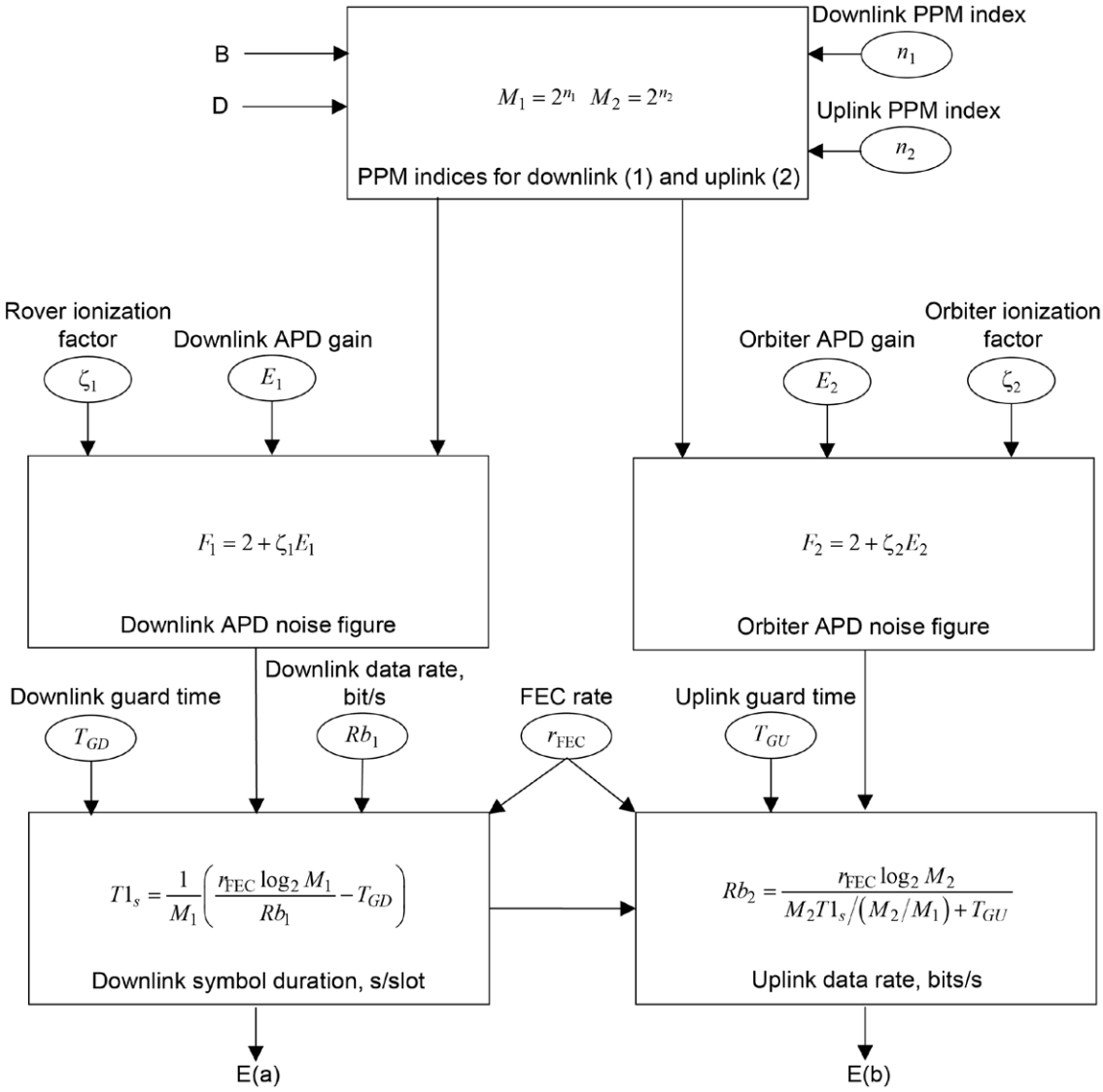

Figure 4.—Modulation scheme included with link results.

Since from here the calculations are the same for each, the variables were generalized accordingly. These are the input variable designations for PPM channel capacity.

$$\text{Variable for capacity calculation} = \begin{Bmatrix} \text{Variable for downlink detector} \\ \text{Variable for orbiter detector} \end{Bmatrix}$$

$$P_s = \begin{Bmatrix} P1_s \\ P2_s \end{Bmatrix} \qquad T_s = \begin{Bmatrix} T1_s \\ T2_s \end{Bmatrix} \qquad R_b = \begin{Bmatrix} Rb_1 \\ Rb_2 \end{Bmatrix}$$

$$D_R = \begin{Bmatrix} D_{\text{det}} \\ D_{\text{orb}} \end{Bmatrix} \qquad \eta_{\text{det}} = \begin{Bmatrix} \eta_{\text{det}1} \\ \eta_{\text{det}\,2} \end{Bmatrix} \qquad T_a = \begin{Bmatrix} T_{\text{Mars}} \\ T_{\text{orb}} \end{Bmatrix}$$

$$I_{Rad} = \begin{Bmatrix} I_{\text{Sky}} \\ I_{\text{Planet}} \end{Bmatrix} \qquad F = \begin{Bmatrix} F_1 \\ F_2 \end{Bmatrix} \qquad M = \begin{Bmatrix} M_1 \\ M_2 \end{Bmatrix}$$

$$E = \begin{Bmatrix} E_1 \\ E_2 \end{Bmatrix}$$

These are the output variable designations for PPM channel capacity.

$$\text{Output variable} = \begin{Bmatrix} \text{variable for downlink detector} \\ \text{variable for orbiter detector} \end{Bmatrix}$$

$$K_s = \begin{Bmatrix} \text{Signal}\left(\dfrac{\text{photons}}{\text{slot}}\right) \text{on downlink} \\ \text{Signal}\left(\dfrac{\text{photons}}{\text{slot}}\right) \text{on orbiter uplink} \end{Bmatrix} \qquad K_b = \begin{Bmatrix} \text{Background}\left(\dfrac{\text{photons}}{\text{slot}}\right) \text{on downlink} \\ \text{Background}\left(\dfrac{\text{photons}}{\text{slot}}\right) \text{on orbiter uplink} \end{Bmatrix}$$

$$\Phi = \begin{Bmatrix} \text{Downlink detector dark noise}\left(\dfrac{\text{counts}}{\text{second}}\right) \\ \text{Orbiter detector dark noise}\left(\dfrac{\text{counts}}{\text{second}}\right) \end{Bmatrix} \qquad K_n = \begin{Bmatrix} \text{Noise}\left(\dfrac{\text{photons}}{\text{slot}}\right) \text{on downlink} \\ \text{Noise}\left(\dfrac{\text{photons}}{\text{slot}}\right) \text{on orbiter uplink} \end{Bmatrix}$$

$$SNR = \begin{Bmatrix} SNR_1 \text{ on downlink} \\ SNR_2 \text{ on orbiter uplink} \end{Bmatrix} \qquad Pbf = \begin{Bmatrix} \text{Bit error rate on downlink} \\ \text{Bit error rate on orbiter uplink} \end{Bmatrix}$$

$$K_{SM} = \begin{Bmatrix} \text{Required}\left(\dfrac{\text{Photons}}{\text{Slot}}\right) \text{to support } Rb_1 \\ \text{Required}\left(\dfrac{\text{Photons}}{\text{Slot}}\right) \text{to support } Rb_2 \end{Bmatrix} \qquad \Lambda_{\text{Unc}} = \begin{Bmatrix} \text{Power margin for downlink} \\ \text{Power margin for orbiter uplink} \end{Bmatrix}$$

$$P_{\text{Rqd}} = \begin{Bmatrix} \text{Power required (watts) on downlink detector to support } Rb_1 \\ \text{Power required (watts) on orbiter detector to support } Rb_2 \end{Bmatrix}$$

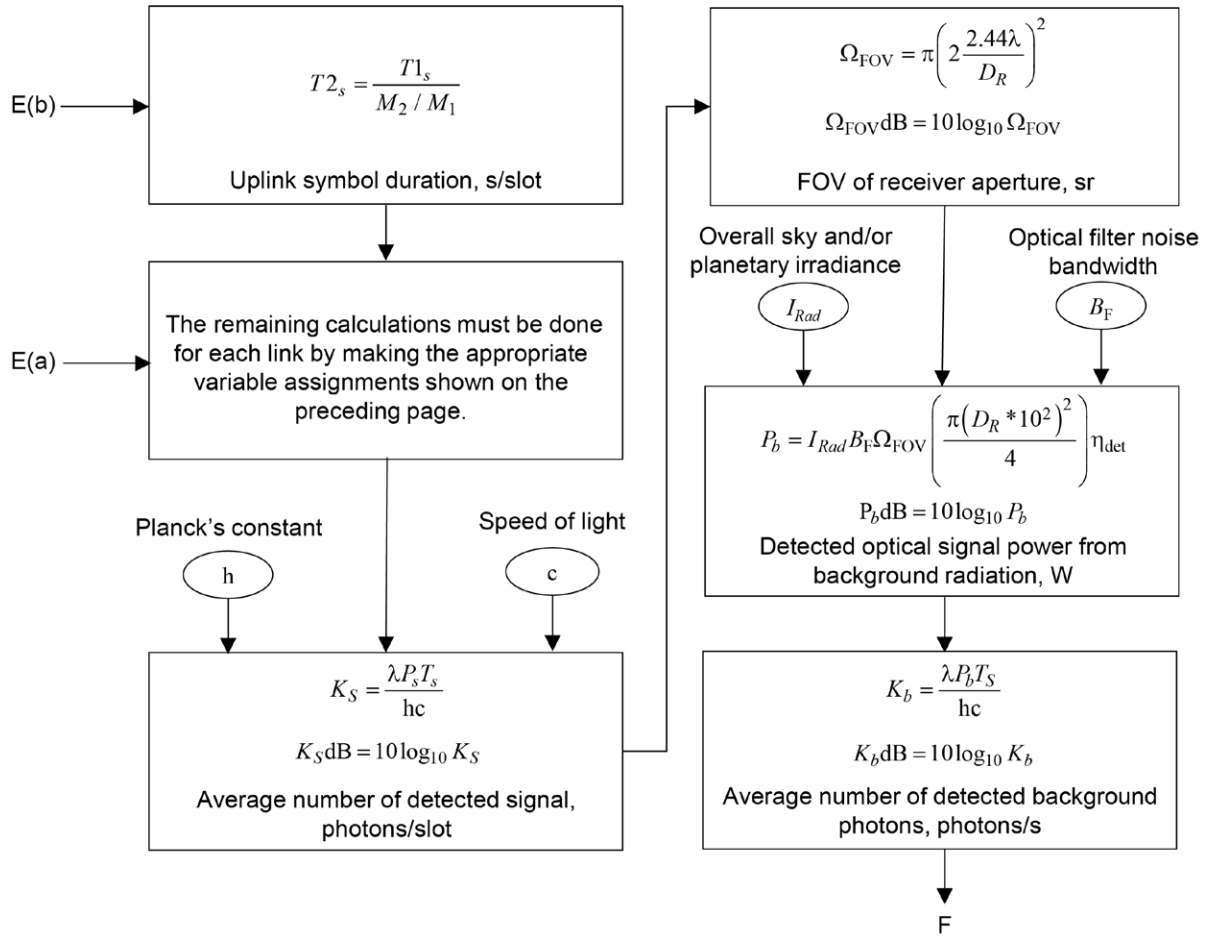

Figure 5.—Background noise and radiation added to detected photons per slot.

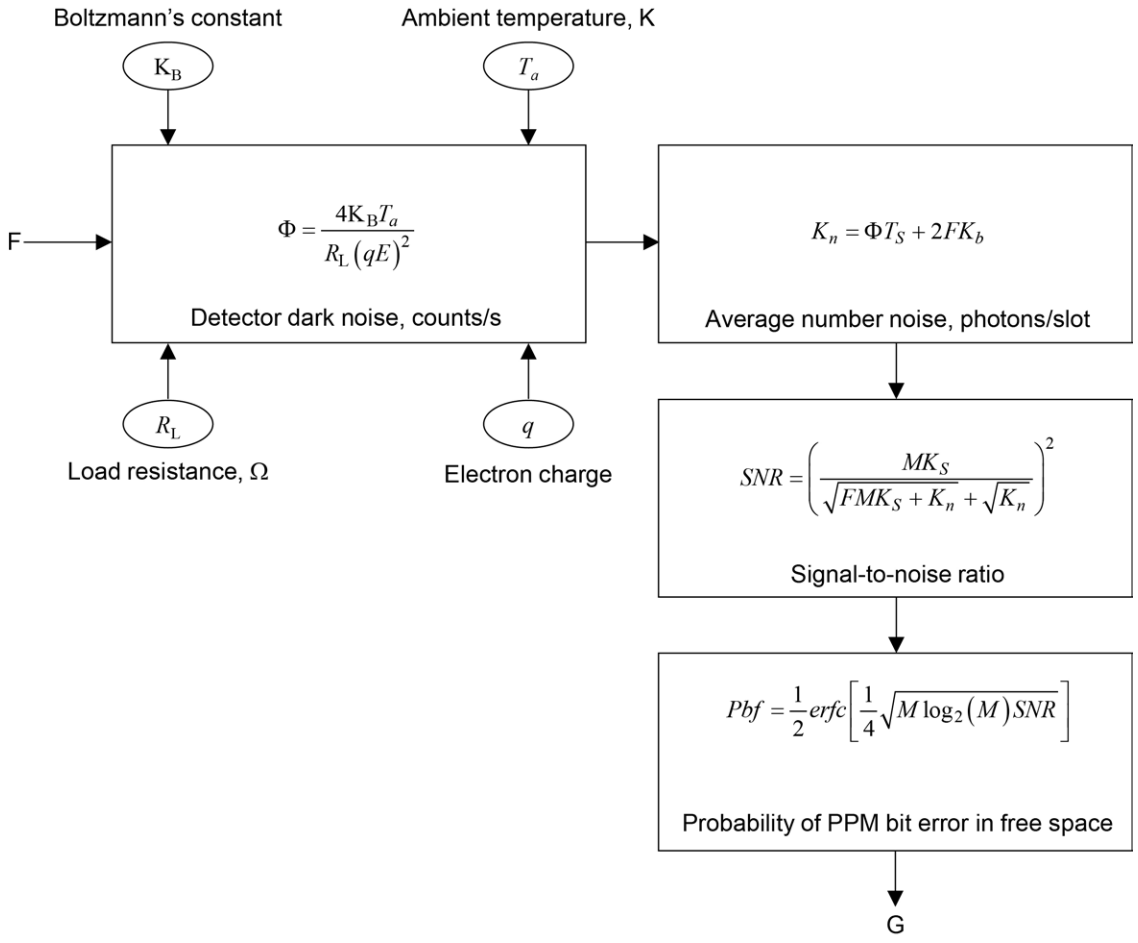

Figure 6.—Link bit error probability from signal-to-noise calculation.

This portion of the flowchart contains the link power margin calculations for the PPM.

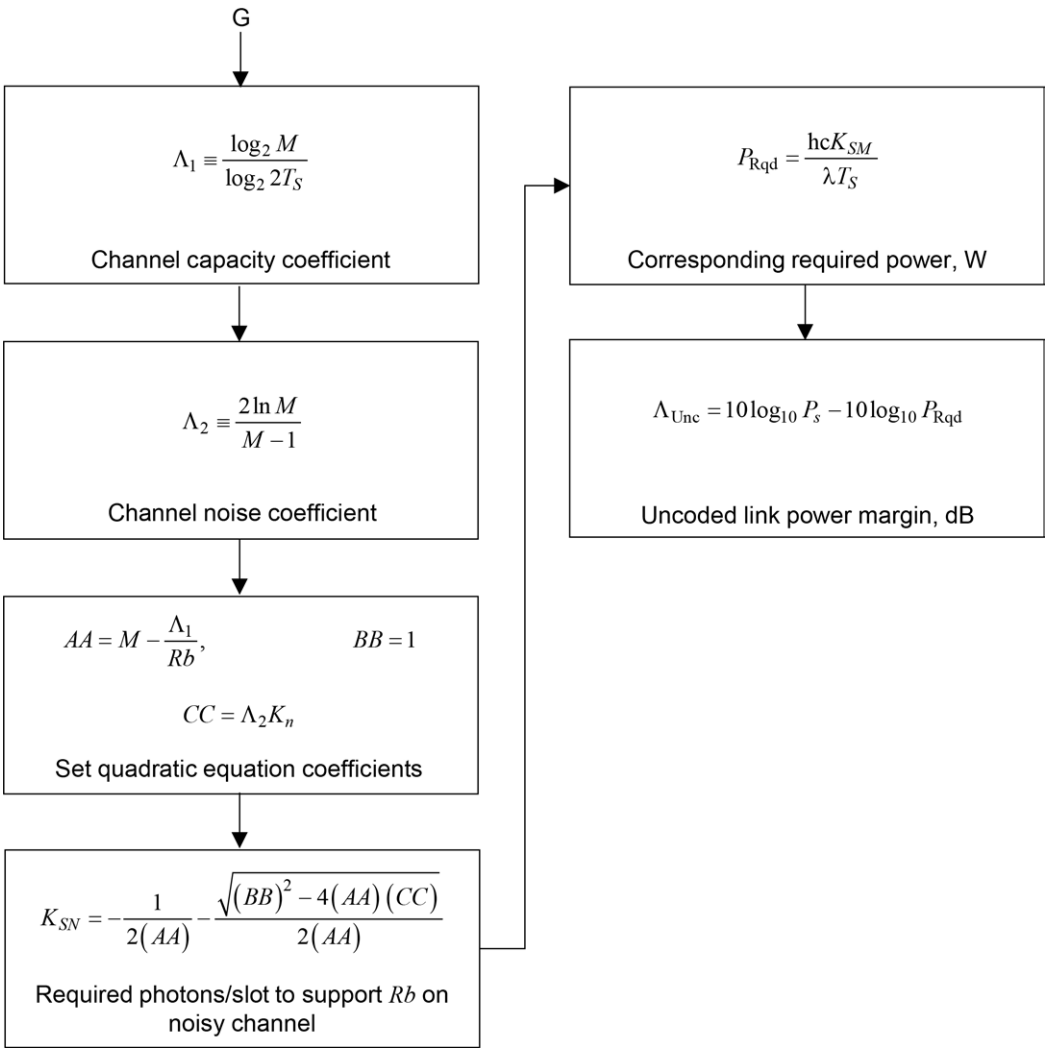

Figure 7.—Link power margin calculations for PPM.

4.0 Conclusion

Duplexing a free-space (FS) optical communication link between an orbiter around Mars and a rover on its surface is possible by utilizing a modulated retro-reflector (MRR). In the proposed scenario setup, the MRR lies on the rover due to power restraints and the laser source is on the satellite. Due to the setup, information, which can be varying types of media, can be sent through both directions of the communication path. By using a MRR, the calculations use pulse-position modulation (PPM) as an alternative modulating scheme to interpret a distorted signal. The arrangement starts as the fundamental PPM scheme and once the MRR affects the link, the scheme switches to a nested-PPM structure. A link budget was derived to show the link characteristics of this system, taking into effect the modulation schemes.

The link budget will help prove that the system's utilization of a FS duplex optical communication link with a MRR will or will not perform in the conditions the user provides. The budget is written

generally to allow flexibility for any system set up with one laser source of power and a MRR. However, since the link budget uses theoretical equations, there is potential discrepancy between the link budget's result and the actual result. This can be due to an added error or human factor. Since data transmission is expensive and sometimes taxing to the system, this link budget will provide useful information for the system's characteristics before sending data up and down its links.

Appendix A.—Nomenclature

AGI	Analytical Graphics, Inc.
APD	avalanche photodiode
BER	bit error rate
FEC	forward error correction
FOV	field of view
FS	free space
MRO	Mars Reconnaissance Orbiter
MRR	modulated retro-reflector
OOK	on-off keying
PPM	pulse-position modulation
PPM2	pulse-position modulation of order 2
PPM4	pulse-position modulation of order 4
RF	radio frequency
SCaN	Space Communications and Navigation
STK	Systems Tool Kit®

Symbols

AA	set quadratic equation coefficient of $M - \frac{\Lambda_1}{Rb}$
B_F	optical filter noise bandwidth
BB	set quadratic equation coefficient of 1
C	channel capacity
C_{PPM}	channel capacity for pulse-position modulation downlink
CC	set quadratic equation coefficient of $\Lambda_2 K_n$
c	speed of light, 299,792,458 m/s
D_{det}	rover detector aperture diameter
D_{MRR}	modulated retro-reflector aperture diameter
D_{orb}	orbiter detector aperture diameter
D_R	detector aperture diameter
D_T	orbiter transmitter aperture diameter
d_{min}	distance between slots
E	avalanche photodiode gain
E_1	rover avalanche photodiode gain
E_2	orbiter avalanche photodiode gain
$EIRP$	effective isotropic radiated power of orbiter optical transmitter
$erfc$	complementary error function
F	noise figure
F_1	downlink avalanche photodiode noise figure
F_2	orbiter avalanche photodiode noise figure
G	gain
G_{det}	receive gain of rover detector
G_{orb}	receive gain of orbiter detector
$Grec_{MRR}$	receive gain of modulated retro-reflector
G_T	orbiter transmitter aperture gain

Gtr_{MRR}	transmit and reflection gain of modulated retro-reflector
h	Planck's constant, $6.62607004 \times 10^{-34}$ m^2 kg/s
I_{Rad}	overall sky and/or planetary irradiance
I_{Rad}MS	solar reflection from Mars surface radiance
K	number of photons
K_B	Boltzmann's constant, $1.38064852 \times 10^{-23}$ m^2 kg s^{-2} K^{-1}
K_b	average number of detected background photons
K_{b1}	average number of detected background photons for downlink
K_{b2}	average number of detected background photons for uplink
K_n	average number noise
K_S	average number of detected signal
K_{S1}	number of photons per slot detected on downlink
K_{S2}	number of photons per slot detected on uplink
K_{SM}	require photons per slot to support uplink or downlink data rate
K_{SN}	required photons per slot to support data rate on noisy channel
k	time slot
L_{FS}	free-space path loss
M	pulse-position modulation index
M_1	pulse-position modulation index for downlink
M_2	pulse-position modulation index for uplink
MT	temporal width
N_{MRR}	number of modulated retro-reflectors
n_1	downlink pulse-position modulation index
n_2	uplink pulse-position modulation index
n^{th}	specific time slot when an error happened
P	power
P_b	detected optical signal power from background radiation
P_{Mars}	communication power available on Mars surface
P_{orb}	communication power available on Mars orbiter
P_{Rqd}	corresponding required power
P_s	detected optical signal power
P_T	orbiter transmitter laser power
$P1_b$	background power for downlink
$P1_s$	detected optical signal power of downlink detector
$P2_b$	background power for uplink
$P2_s$	detected optical signal power on orbiter
Pbf	probability of pulse-position modulation bit error in free space
$Pmrr_s$	detected optical signal power of modulated retro-reflector
$Pmrr_T$	modulated retro-reflector transmitted signal power
Pr	average power
q	electron charge
R_L	load resistance
Rb	data rate
Rb_1	downlink data rate
Rb_2	uplink data rate
Rng	range between orbiter and modulated retro-reflector on Mars

r	distance traveled
r_{FEC}	forward error correction rate
S_R	modulated retro-reflector reflection Strehl ratio
SNR	signal-to-noise ratio
SNR_1	signal-to-noise ratio for downlink
SNR_2	signal-to-noise ratio for uplink
T	slot time interval
T_a	ambient temperature
T_G	guard time interval
T_{GD}	downlink guard time
T_{GU}	uplink guard time
T_S	symbol duration
T_{S1}	slot time interval for downlink signal
T_{S2}	slot time interval for nested uplink signal
$T1_S$	downlink symbol duration
$T2_S$	uplink symbol duration
ζ_1	rover ionization factor
ζ_2	orbiter ionization factor
η_B	bandwidth efficiency
η_{det}	quantum efficiency of detector
η_{det1}	quantum efficiency of rover detector
η_{det2}	quantum efficiency of orbiter detector
η_P	power efficiency
θ	angle in radians
θ_{div}	transmitted beam divergence angle
Λ_1	channel capacity coefficient
Λ_2	channel noise coefficient
Λ_{Unc}	uncoded link power margin
λ	operating laser wavelength
σ_λ	modulated retro-reflector reflective surface roughness
τ_{atm}	atmospheric absorption and scattering scenario specific
$\overline{\tau_{atm}}$	atmospheric absorption and scattering overall
$\tau_{atm}(\theta)$	atmospheric absorption and scattering angle specific
τ_T	total optical losses in transmitter
Φ	detector dark noise
Ω_{FOV}	field-of-view of receiver aperture

Appendix B.—Pulse-Position Modulation (PPM), Guard Time, and Nested PPM Overview

On-off keying (OOK) is the most used modulation technique reported in optical communications. OOK is used for its simplicity because it is represented by an optical pulse, sourced from laser or other medium, which conveys what data value was transmitted. If there is an absent optical pulse for a duration, it is denoted as a binary zero, whereas if there was a pulse (meaning a source of power was detected from the given medium), it represents a binary one. A modulation scheme that uses the basis of OOK is called PPM. This scheme improves the power efficiency that OOK provides, but at the expense of higher complexity. Nevertheless, PPM is widely used in applications that require lower power consumption like deep space laser communications and handheld devices.

In contrast to OOK, PPM provides free-space (FS) optics a method to transmit data in an orthogonal modulation technique. This is accomplished by representing the information within fixed timeframes that are equidistant in the form of pulses. Depending on what PPM index (M) the system is utilizing, it will change the number of available transmitted slots there are to make the combination of pulses a certain value or letter. With n being the bit resolution, the modulation index is found by

$$M = 2^n \tag{39}$$

To symbolize the modulation index with PPM, it can be written in two forms: M-PPM or M trailing after PPM directly. For example, PPM2 is formally written as PPM with a modulation index of two. When the modulation index is two, it means that the slots are viewed 0 or 1, which is also known as binary. Figure 8 shows only two slots that can contain data to illustrate PPM2. These slots are of equal length because each pulse is the same amplitude and width. For all general PPM signals, the distance can be found with

$$d_{\min-\mathrm{PPM}} = 2MP^2 \log_2\left(\frac{M}{Rb}\right) \tag{40}$$

where P is the power in watts and R_b is the achievable data rate. Equation (40) comes from signal theory and a more indepth explanation is provided in Reference 7. The relative placement of the on-off pulses in each slot dictates the value being sent.

For further clarification, if the letter H was sent, the pulses should read 01001000 per the ASCII table for binary conversion. For this example, the first slot will be designated to remain zero, resulting in Figure 9.

Here, every two slots were joined with a longer division to emphasize the symbol time, which is the grouping that contains one pulse with a flat line that designates no pulse received. A clearer representation of the terminology is shown in Figure 10. Recall that this example is showing PPM2; it is possible to increase the number of slots if the arrangement requires it by increasing the modulation index as denoted in Equation (39).

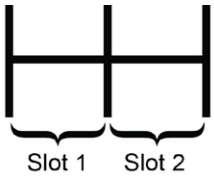

Figure 8.—Slot representation for pulse-position modulation of order 2.

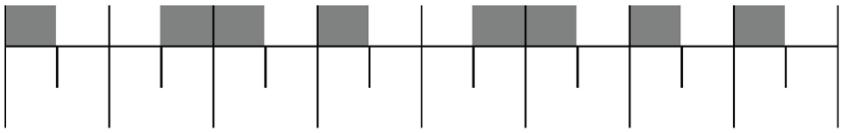

Figure 9.—First slot designation of zero example with letter H sent.

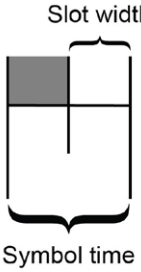

Figure 10.—Slot width and symbol time.

Due to the fixed slot widths, the duty cycle is also fixed. This occurs at $M - 1$, which forces each pulse to have amplitudes of MPr, where Pr is average power, to maintain the average optical power of Pr. If the system does not utilize rectangular-shaped pulses, this may not be the case. PPM also has a low signal-to-noise ratio (*SNR*) with a bandwidth efficiency of

$$\eta_B = \frac{RbM}{\log_2 M} \tag{41}$$

and a power efficiency of

$$\eta_P = P - 5\log_{10}\left[\left(\frac{M}{2}\right)\log_2 M\right] \tag{42}$$

(see Ref. 7 for more details if needed). Since there are no ideal systems, PPM has three types of errors in the isochronous schemes. These are

(1) An erasure error that can happen by transmitting a pulse not detected on the receiving node
(2) A false alarm error where a transmitted zero is falsely detected as a one in the $(k + n)^{th}$ slot
(3) A wrong slot error that happens when the pulse is detected in the slot adjacent to it

Subsequently, a single slot error can only affect a total of log2M bits. When a false alarm error happens, it divides a symbol into two, leading to timing issues. For example, since slots can be close together, and are usually in the nanosecond duration range, photons may run over into the next slot. If the photons run over, then there may not be enough space for the system to see and fix the error. Nevertheless, there is a way to separate the bits sent by integrating guard time into the system.

Guard time is simply a pulse that, on detection, is automatically assigned to zero regardless of whether the receiver detected signal power or not. The system will essentially do nothing within that guard time period; its main purpose is to keep the detector on track. Instead, it will restart the time to decide if a zero or a one was received. Guard time can be the same slot width as a standard pulse in the one or zero slot or a factor longer or a fraction shorter than the normal slot being used to transmit data. By including guard time, the symbol time increases by the length and amount of guard times used within a symbol time. Figure 11 shows a guard slot at the beginning with a zero and then a one that was transmitted. The guard slot is the darker of the two pulses and the lighter is the data transmitted. However, the system can have a guard slot anywhere in the system, including at the end. The definitions are described in Figure 12.

From Figure 11, the bits per symbol continue to be one. However, if the system requires a higher modulation index or more bit per symbols sent within each symbol time, the relationship can be found with Equation (39). If guard time were to be included, please reference Table I for the usual number of guard slots used.

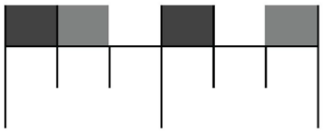

Figure 11.—Guard slot beginning with transmitting a zero and then transmitting a one.

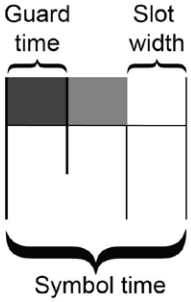

Figure 12.—Guard time, slot width, and symbol time.

TABLE I.—TYPICAL NUMBER OF GUARD SLOTS BASED ON PULSE-POSITION MODULATION (PPM) ORDER AND BITS PER SYMBOL (REF. 8)

Bits per symbol	PPM order, modulation index (*M*)	Guard slots
2	4	1
3	8	2
4	16	4
5	32	8
6	64	16
7	128	32

In the case of nested PPM, all the fundamentals are identical. However, the algorithm at the result will need to decipher the originally transmitted data from the full received waveform. This way, the system can identify the received data from the second or middle source. In terms of the scenario described in this paper, the orbiter sends down information slower than what the modulated retro-reflector (MRR) will transmit back up. This is essential, because if the MRR transmits slower than the orbiter's laser pulses, the MRR will run out of time and power to transmit data. In consideration of the foregoing, the orbiter and MRR are able to send the same data rate or different data rates. The way to create different data rates is by sending more data in one pulse of the orbiter's pulse, and instead of having a one-to-one ratio for symbol times factored together, add more symbol times within the one symbol time that the orbiter sent down. However, the higher the data rate used in the system, the fewer photons will be sent out. This may not be an issue for high power or short-distance systems, but noise still plays a large role. In Figure 13, an example of the scenario with random sent values is shown. In this example, the orbiter transmits a zero and then a one in a continuous loop with the MRR sending parsed data in the sets 001 110. It must be noted that even if the initial source has no data to be sent, the orbiter still must send a dummy value or a straight pulse so there is available power for the second source to use. In Figure 13, the first two lines of data represent a fundamental PPM scheme, whereas the last signal, named "received signal on orbiter," represents nested PPM. This was all done with PPM2 with a slot of guard time.

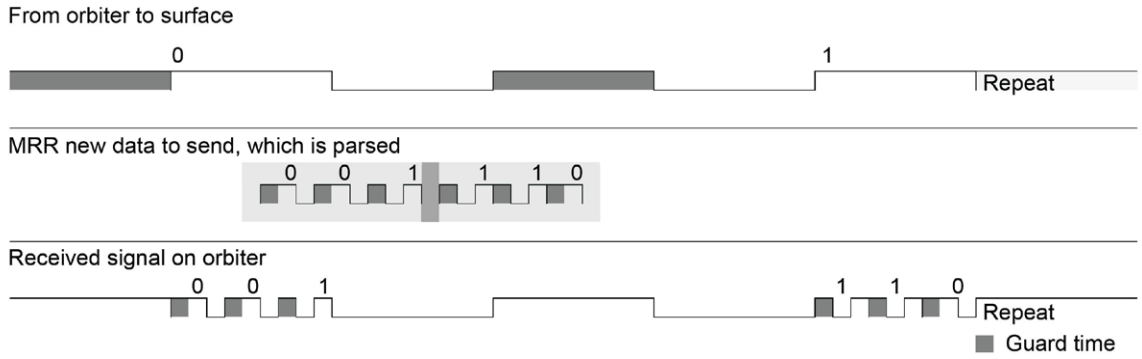

Figure 13.—Fundamental pulse-position modulation (PPM) versus nested-PPM scheme.

References

1. Manning, R.M.: SCaN Optical Link Assessment Tool Version 3. User's Guide, Part 2: The Physical Basis for the Calculations. https://software.nasa.gov/software/LEW19463-1 Accessed Sept. 27, 2018.
2. Rabinovich, W.S., et al.: Free-Space Optical Communications Link at 1550 nm Using Multiple-Quantum-Well Modulating Retroreflectors in a Marine Environment. Opt. Eng., vol. 44, no. 5, 2005.
3. Serra, Paul; Barnwell, Nathan; and Conklin, John W.: A Novel, Low Power Optical Communication Instrument for Small Satellites. Proceedings of the 29th Annual AIAA/USU Conference on Small Satellites, SSC15–V1–10, 2015.
4. Biswas, A.; and Piazzolla, S.: Deep-Space Optical Communications Downlink Budget From Mars: System Parameters. IPN Progress Report 42–154, 2003.
5. Ortiz, Gerardo G.; Sandusky, John V.; and Biswas, Abhijit: Design of the Opto-Electronic Receiver for Deep Space Optical Communications. SPIE Proceedings, vol. 3932, paper 13, 2000.
6. Gagliardi, Robert M.; and Karp, Sherman: Optical Communications. Second ed., Ch. 6, Wiley, New York, 1995.
7. Ghassemlooy, Z.; Popoola, W.; and Rajbhandari, S.: Optical Wireless Communications. Ch. 4, CRC Press, Boca Raton, FL, 2013.
8. Nappier, J.: Optical Waveform Analysis. Oct. 2015.